Ultrafast Transient Infrared for Probing Trapping States in Hybrid Perovskite Films

Ahmed M. El-Zohry[a,d*], Bekir Türedir[b], Abdullah Alsalloum[b], Partha Maity[a], Osman M. Bakr[b], Boon S. Ooi[c], and Omar F. Mohammed[a*]

[a] King Abdullah University of Science and Technology (KAUST), Division of Physical Sciences and Engineering, Thuwal 23955-6900, KSA.
[b] KAUST Catalysis Center, King Abdullah University of Science and Technology (KAUST), Thuwal 23955-6900, Saudi Arabia..
[c] Photonics Laboratory, King Abdullah University of Science and Technology (KAUST), Thuwal 23955-6900, KSA.
[d] Department of Physics, AlbaNova Center, Stockholm University, 10691 Stockholm, Sweden.
*Corresponding author: amfzohry@yahoo.com, omar.abdelsaboor@kaust.edu.sa

Abstract

Studying the charge dynamics of perovskite materials is a crucial step to understand the outstanding performance of these materials in various fields. Herein, we utilize transient absorption in the mid-infrared region, where solely electron signatures in the conduction bands are monitored without external contributions from other dynamical species. Within the measured range of 4000 nm to 6000 nm (2500-1666 cm^{-1}), the recombination and the trapping processes of the excited carriers could be easily monitored. Moreover, we reveal that within this spectral region the trapping process could be distinguished from recombination process, in which the iodide-based films show more tendencies to trap the excited electrons in comparison to the bromide-based derivatives. The trapping process was assigned due to the heat release in the mid-infrared region, while the traditional band-gap recombination process did not show such process. Various parameters have been tested such as film composition, excitation dependence and the probing wavelength. This study open new frontiers for the transient mid-infrared absorption to assign the trapping process in perovskite films both qualitatively and quantitatively.

Introduction:

Hybrid perovskite materials have recently attracted lots of attention due to their unique photo-physical properties and their high performances in various applications such as solar cells and light emitting diodes.[1-13] However, still controlling the amount of traps present in these materials especially upon making thin films relevant for various applications is a challenging procedure.[14-15] The presence of trap states either through structural defects or other types can quench the charge carriers motilities inside the materials and thus reducing both the device's performance and its stability.[8, 14, 16-18] Various direct and indirect methods have been applied to track and quantify trap states such as electrical or optical measurements, however, most of these still have some drawbacks.[8, 14-19] For instance, conductivity measurements have low time resolutions and can't distinguish between various carriers such as electrons and holes especially upon having

close motilities.[20] Also, the most commonly used optical measurements such as time-resolved photoluminescence or transient absorption in the visible range couldn't afford direct spectral signatures for trapping states except providing variations of multi-exponential kinetic rates between different samples according to the estimated traps present in the investigated samples.[1-2, 7, 13, 21-23] Also, no direct spectral information could be drawn between the presence of trap states and their influence on the charge mobility. Thus, still there is a need for a direct transient optical method to track and quantify the trapping process in perovskite materials, and correlate their presence directly on charge dynamics. For that sake, we utilized infrared probe to monitor the charge dynamics of four different perovskite films. Following the charge dynamics using fs-TA in the mid-IR has been used previously for several systems including metal complexes[24-27], organic dyes[28-33], metals[34], and semiconductors[17, 20, 35-38]. Basically for semiconductors, the electron's absorption in the conduction band with high density of states has a broad spectral signature extending from 3,333 nm (3000 cm^{-1}) to 11,111 nm (900 cm^{-1}), in which other contributions from cationic or anionic molecular species present can be easily quantified.[20, 24, 28-29] The positive signature in the mid-IR upon photon excitation is ascribed to the presence of intra-transition of free electrons in/into the conduction band of the semiconductor used.[20, 39] The transient mid-IR was used to follow trapped electrons at the mid-gap shallow states in the platinized TiO_2 system, in which IR emission (heat) is evolved in the IR region as a result of electron trapping process.[20] Recent mid-IR studies have been done on perovskite materials, however in those studies the authors focused on following the NH vibrational modes, present in the organic cationic part of the perovskites.[16-17, 21, 40] In contrast, in our selected mid-IR region, we don't have any contribution of the vibrational modes of the organic part, only transient signal of electrons in the conduction band.

Herein, we propose using femtosecond transient absorption in the mid-infrared region (fs-TAIR) as a sensitive tool to follow the presence of traps in hybrid perovskite films. In the current study, various hybrid perovskite films have been synthesized and utilized to study the charge dynamics in the mid-IR region extending from ca. 4000-6000 nm (2500-1666 cm^{-1}). It is worth mentioning that in the current study the overall comparison between films is not valid and the same film should be understood under the same measuring conditions. Also, the lifetimes are not the main parameters herein to follow rather than the fundamental understandings for the nature of the

observed signals in this mid-IR region. Thus, we present the fs-TAIR as a potential transient optical tool towards deeper understandings of charge dynamics in perovskite films.

Results and Discussions

The range of current mid-IR fs-measurements is between 2500-1660 cm^{-1}, and perovskite films show no characteristic features in this range. Therefore, any signal for excited perovskite films show represented by a positive transient absorption due to presence of electrons in the CB, as mention earlier. Figure 1A shows the false 2-D plot fs-TA in the mid-IR region with a central detection window of 5000 nm (2000 cm^{-1}) for $MAPbBr_3$ thin film using excitation wavelength of 530 nm. At time zero, an intense positive signal appears due to the population of electrons in the conduction band. [24, 28, 41] This transient positive signal decays exponentially towards zero within few nanoseconds. However, the extracted spectra show negative features at longer time scale > 1.0 ns; see Figure 1B. Also, the extracted kinetic trace at 4900 nm shows a multi-exponential decay for the positive signal with an average lifetime of 120 ps, followed by a small negative feature beyond 2 ns; see Figure 1C. The same film was measured by fs-TA in the visible range, and an extracted kinetic trace at 550 nm corresponding to the ground state bleach (GSA) is compared with the extracted kinetic trace at 4900 nm from the mid-IR region; see Figure 1D. The comparison shows that both normalized kinetic traces from different spectral regions are very similar, except the presence of a new feature at the extracted kinetic trace from the mid-IR range; see Figure 1C-D. The similarity between the two kinetic traces for $MAPbBr_3$ film confirms the validity of mid-IR signal to trace charge dynamics in perovskite films. However, the charge dynamics at in the mid-IR region are not similar. For example, negative features at the red-part of the false 2D plot in Figure 1A, appears differently than in the blue-part. Extracting a kinetic trace at 5120 nm (1953 cm^{-1}) shows earlier conversion of positive to negative signals at ca. 100 ps; see Figure 1C. Also, comparing this kinetic trace with the one extracted from the GSB in the visible region, shows different behavior than kinetic trace at 4900 nm; see Figure 1D. This highlights the dependence of such negative feature on the probed window.

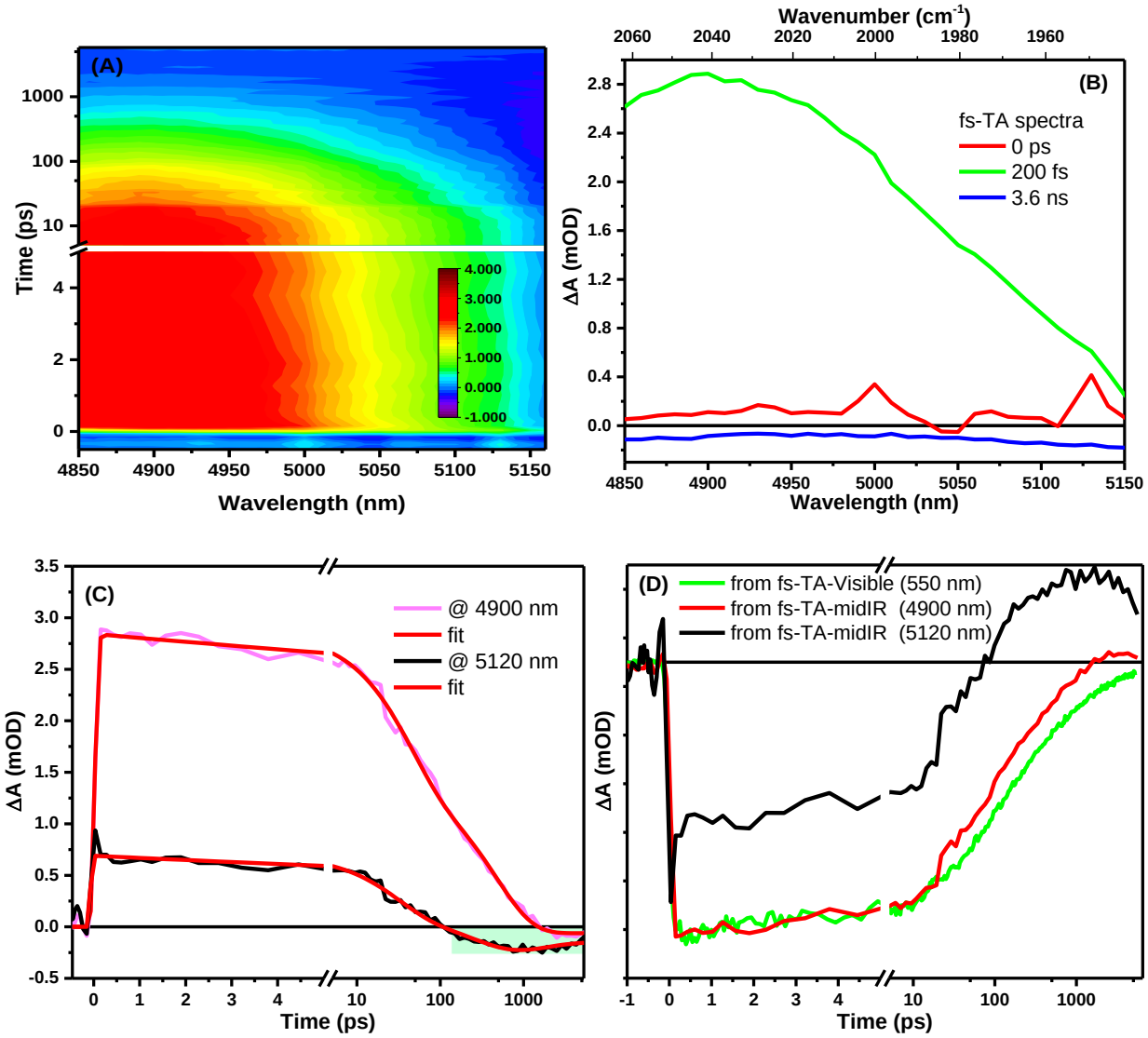

Figure 1: (A) 2D-false color plot for fs-transient absorption in the mid-infrared regions for $MAPbBr_3$ film using 530 nm as an excitation source. (B) Extracted spectra for transient spectra in mid-infrared region, the spectra are corrected for the wavelength scale. (C) Extracted kinetic trace at 4900 and 5120 nm with corresponding fitting, green shaded area highlights the negative signal. (D) Comparison between normalized kinetic traces in the infrared and visible ranges for $MAPbBr_3$ film.

Upon measuring the iodide-derivative, $MAPbI_3$ film, a detectable fs-TA mid-IR signal was also found. However, interestingly, the transient mid-IR signal for $MAPbI_3$ film was changing during measurements over minutes time scale; see Figure 2A. Thus, various kinetic traces were extracted from each scan and compared to later scans. For instance, the fresh-irradiated film (0 min.), appositive signal was measured until ca. 100 ps, and then a small negative signal started to emerge. The disappearance of the positive signal became faster with the longer the exposure process associated with an increase of the signal at early times; see Figure 2A . For example, at

26 minute of irradiation, the positive signal converted into a negative signal within 10 ps; see Figure 2A. Interestingly, this process is reversible, in which switching off the irradiation for almost 8 minutes, and re-measure the dynamics again at the same irradiated spot (34 min. in the figure), the dynamics slowly started to be similar to the 10 minutes measurements; see Figure 2A. Upon measuring the same film in the visible range, a strong GSB signal at ca. 760 nm was observed overlapping with an ESA spectra extending from 650 to 850 nm. However, no change in dynamics has been observed in the visible range similar to the shown data in the mid-IR range. And upon comparing the extracted normalized visible kinetic trace at 760 nm with the ones from the mid-IR, it is evident the visible kinetic trace is similar to the one from mid-IR at 26 min only at early times; see Figure 2B. However, still at later times, the mid-IR signal switches its sign, but not the visible kinetic trace at 760 nm. The change of charge dynamics upon irradiation has been assigned in iodide-rich perovskite materials to halide-defects assisted by the low energy needed for defects formation.[42-43] This highlights that this appearance of negative features is a dynamical process. Additionally, the extracted kinetic trace at 4900 nm from the $MAPbI_3$ shows stronger and earlier negative signal than in $MAPbBr_3$. Also, for further confirmation for the working conditions, a reference of silicon wafer substrate was measured under the same procedure, and no negative features have been detected. Thus, we assign these strong negative signatures in the mid-IR for $MAPbI_3$ film to the trapping process, in which the mid-IR signal is more sensitive than in the visible range. Several studies showed that iodide based perovskites are more vulnerable for formation of more trap states than bromide ones.[1, 8, 14, 23]

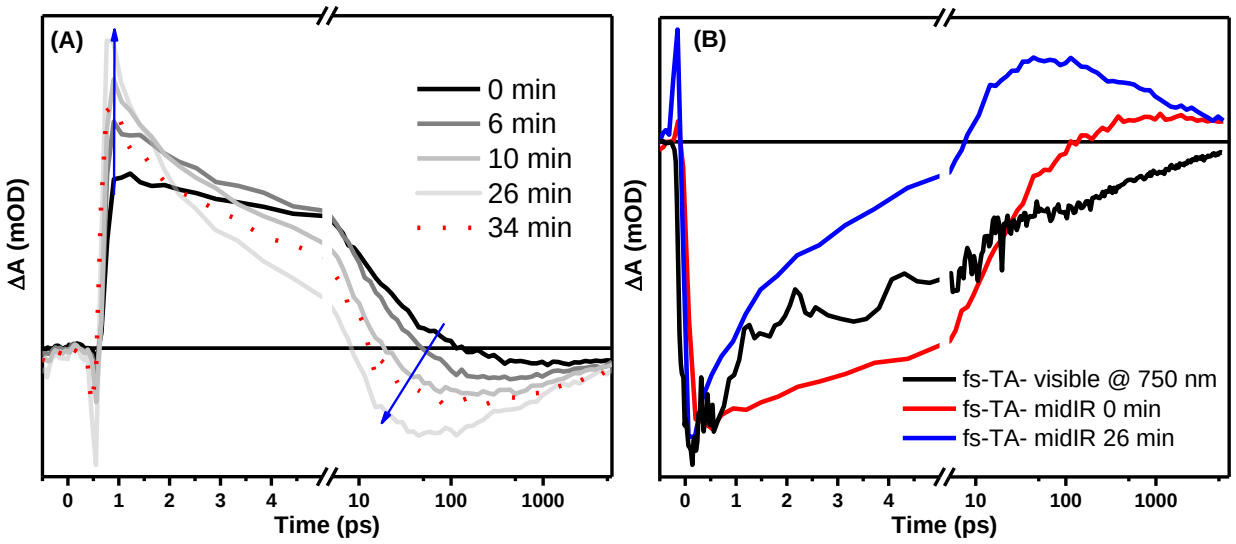

Figure 2: (A) Extracted kinetic trace at 4900 nm at different irradiation time shown in minutes for $MAPbI_3$ film, using 520 nm with excitation power of 500 µW. (B) Comparison between normalized kinetic traces in the infrared and visible ranges for $MAPbI_3$ film.

To scrutinize our interpretation about the sensitivity of mid-IR towards trapping process, we performed the same measurements on other perovskite films including $FAPbBr_3$, $FAPbI_3$ and mixture of their halides. For $FAPbBr_3$, the mid-IR signal shows primarily a strong negative signal close to time zero converting into a positive signal with a lifetime of ca. 60 fs, which has been assigned to the exciton thermalization[7]/dissociation process; see Figure 3A-B. In $MAPbBr_3$, exciton binding energy seems to be smaller, thus, no detection of exciton dissociation process could be seen; see Figure 1. Then the charge recombination process has been fitted with multi exponential behavior, giving an average lifetime is about 10 ps, see Figure 3B. For $FAPbI_3$ film, similar observation was estimated for the lifetime needed for exciton dissociation in $FAPbI_3$ film; see Figure 3C-D. However, instead of charge recombination, the signal converted again to a negative signal due to a trapping process of time component ca. 8.5 ps; see Figure 3D. Then the trapped electrons recombine slowly with a lifetime higher than 1 ns. It is clear that this negative signature in the mid-IR range is associated with the iodide derivative of hybrid perovskite films due to the presence of trapping centers in the iodide perovskites more than in bromide perovskites.

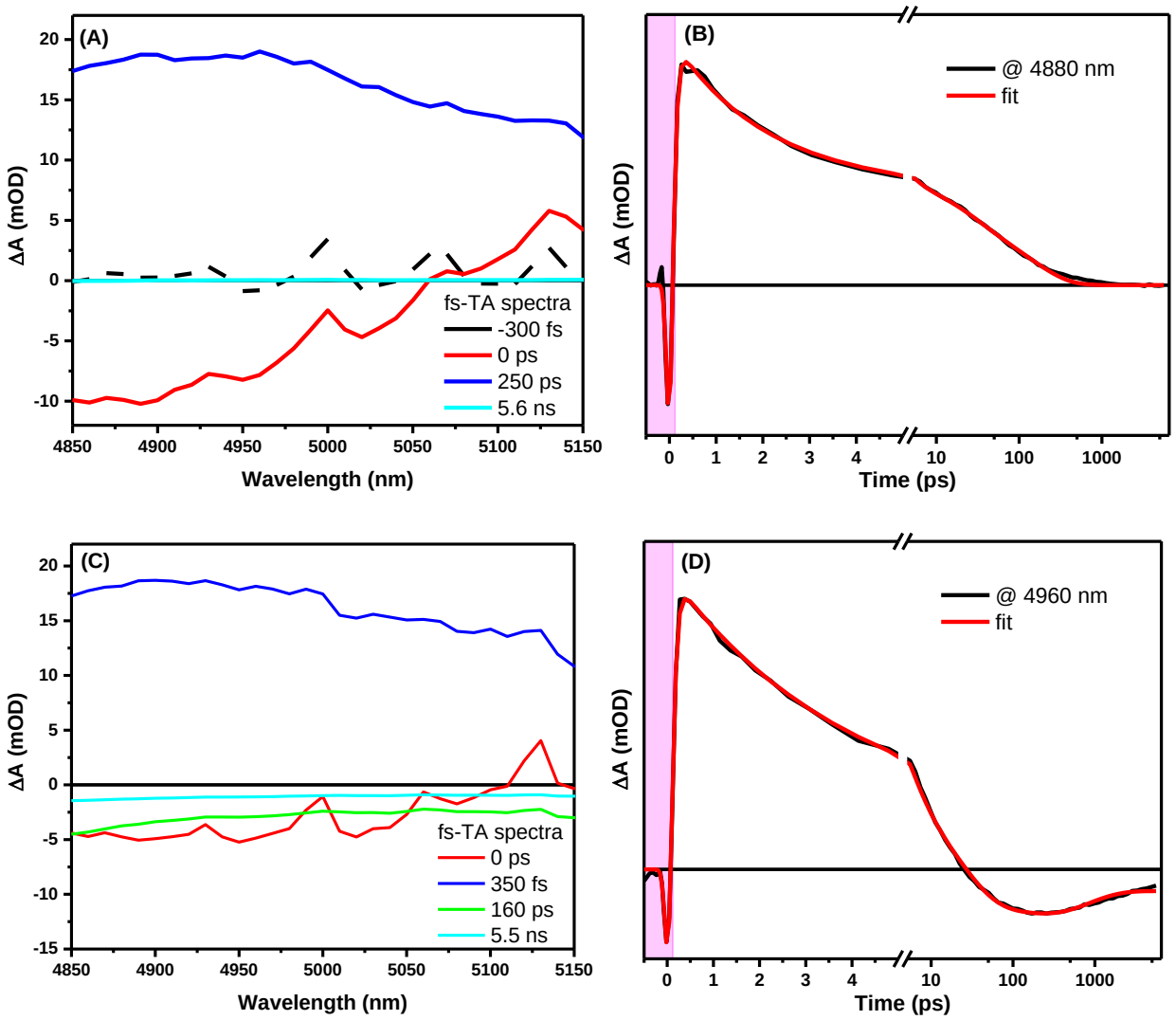

Figure 3: (A) Extracted spectra for transient spectra in mid-infrared region for $FAPbBr_3$ film. (B) Extracted kinetic trace at 4900 nm for $FAPbBr_3$ film. (C) Extracted spectra for transient spectra in mid-infrared region for $FAPbI_3$ film. (B) Extracted kinetic trace at 4900 nm for $FAPbI_3$ film.

We also synthesized other set of various perovskite films of different ratios between the iodide and bromide halides ($MAPbI_nBr_{3-n}$) to investigate the effect of doping with Br ions on the detection of trapping process, and the presence of such negative signal. Figure 4A shows the normalized kinetic traces of mid-IR signals for four films of $MAPbI_nBr_{3-n}$, in which n varies from 0 to 3. The kinetics are similar till ca. 100 ps, then the negative signals appear depending on the amount of iodide halide present. Figure 4B, shows a zoom scale on the negative signal, and it can be shown that pure Br-perovskite has almost no negative signal, and the amplitude of the negative signals are associated with the increase of iodide content.

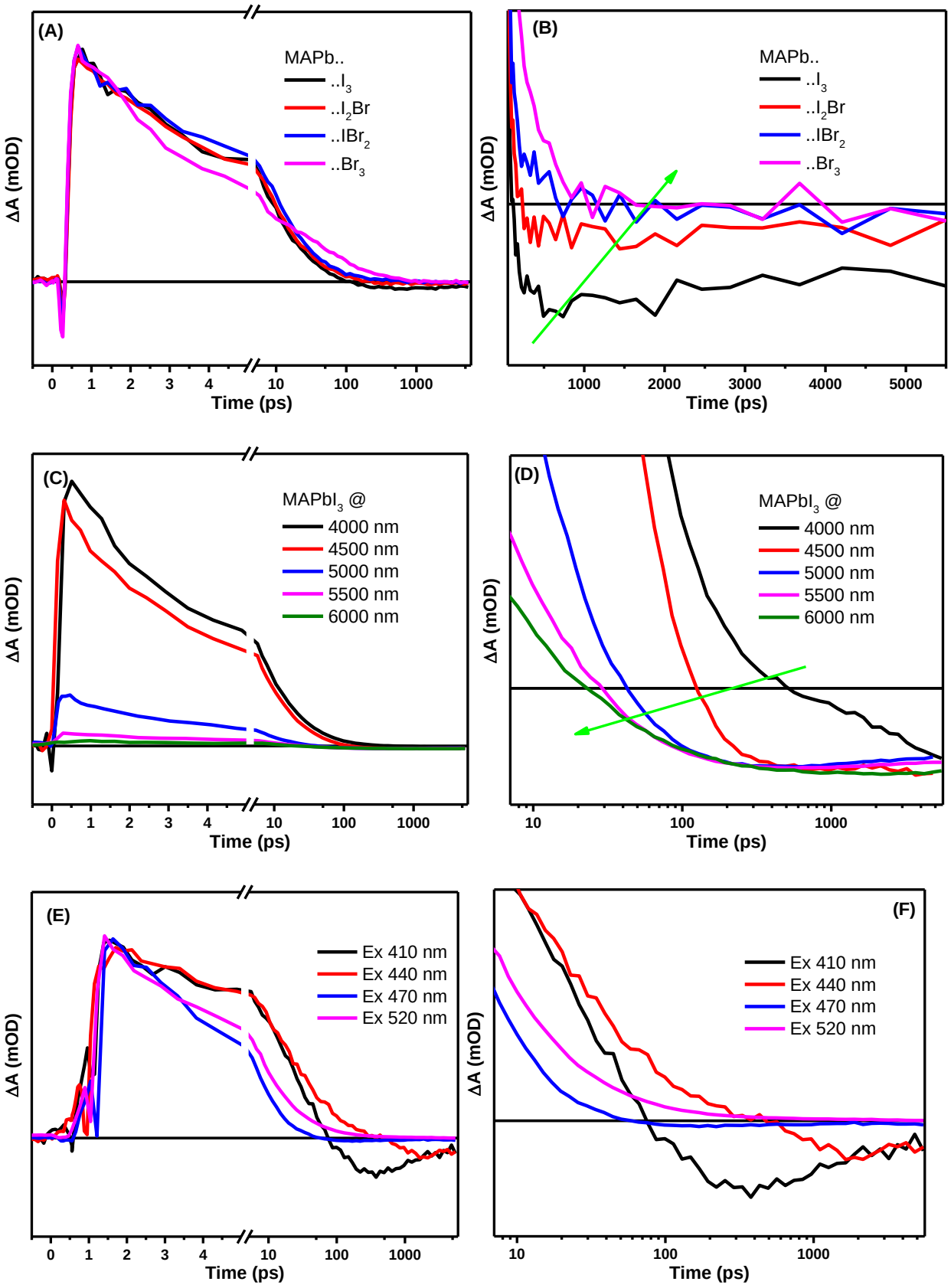
(A)
MAPb..
..I3
..I2Br
..IBr2
..Br3
ΔA (mOD)
Time (ps)
(B)
MAPb..
..I3
..I2Br
..IBr2
..Br3
ΔA (mOD)
Time (ps)
(C)
MAPbI3 @
4000 nm
4500 nm
5000 nm
5500 nm
6000 nm
ΔA (mOD)
Time (ps)
(D)
MAPbI3 @
4000 nm
4500 nm
5000 nm
5500 nm
6000 nm
ΔA (mOD)
Time (ps)
(E)
Ex 410 nm
Ex 440 nm
Ex 470 nm
Ex 520 nm
ΔA (mOD)
Time (ps)
(F)
Ex 410 nm
Ex 440 nm
Ex 470 nm
Ex 520 nm
ΔA (mOD)
Time (ps)

Figure 4: Dependence on chemical composition: Normalized kinetic traces extracted form $MAPbI_nBr_{3-n}$ films using 520 nm as excitation (A), zoomed area for the same plot showing the appearance of negative signals (B). Dependence on mid-IR detection window: Normalized kinetic traces for $MAPbI_3$ film under excitation of 520 nm and at different probing wavelengths (C), zoomed in area for the same plot showing the appearance of negative signals (D). Dependence on excitation wavelengths: Normalized kinetic traces for $MAPbI_3$ film under various excitation wavelengths (E), zoomed in area for the same plot showing the appearance of negative signals (F).

To study the dependence of appearance of these negative signals that are associated with the trapping process, we excited the $MAPbI_3$ film by the 520 nm (300 µW), and collected the mid-IR signals at different wavelengths starting from 4000 nm to 6000 nm, as shown in Figure 4C-D. Firstly, the signal is maximized at 4000 nm and gradually declining towards 6000 nm, indicating that at least within our range, using 4000 nm is more appropriate to detect the electrons in the CB for perovskite films; see Figure 4C. Secondly, the appearance of negative signal is faster as soon as going from 4000 nm (2500 cm^{-1}) to 6000 nm (1666 cm^{-1}), in which the switching points happen at ca. 500 ps when using 4000 nm and at ca. 20 ps upon using 6000 nm as a probing IR. These data presents the influence of the energy carried by the probing photons to free the trapped electrons. For instance, the probed pulse at 2500 cm^{-1} can liberate the trapped electron more efficient than 1666 cm^{-1}, and the appearance of negative signal upon using 4000 nm (2500 cm^{-1}) will not appear unless the electron is deeply trapped. In the same way, the appearance of negative signal at 6000 nm (1666 cm^{-1}) is much faster due to lower energy carried by the probe pulse to liberate the trapped electron. These observations are consistent with a previously proposed mechanism that trapped electrons can be excited thermally if the energy difference between the trap state and the CB is small, < 50 meV.[20] This illustrates the incapability of visible probe light to directly track the trapping process due the high energy carried by the photons used.

Furthermore, by changing the excitation wavelength from 410 nm to 520 nm for a new $MAPbI_3$ film, the normalized kinetic traces at 4500 nm show a dependence of the kinetic decay and the wavelength used; see Figure 4E. The appearance of negative signal is faster upon using 410 nm then became slower with 440 nm. Using 470 nm and 520 nm excitation light show very weak signature of negative signal, despite that higher power was used, almost 20 times higher (300 µW) than in 410 nm, that are reflected in faster decays observed upon using 470 and 520 nm; see Figure 4E-F. These excitation dependence shows that the higher the electron can be promoted the higher than chances to be trapped.

From the above transient measurements, the following mechanism can be drawn. From the transient mid-IR data, the iodide perovskite films show more potential to form trap states than

the bromide derivatives, in which the iodide films show more negative IR signal due to the evolved heat produce upon carrier trapping process. Upon using higher band-gap excitations, the probability of electron trapping is increased despite the fluences used, matching with the expected distribution for the states of trap-density present. More importantly, we show a relation between the energy of the probed IR light and the evolution of the negative IR signal, in which the smaller the energy of the probed mid-IR, the weaker the ability of the probed light to liberate the trapped carriers, thus, producing more negative signals that were highlighted in the extracted kinetic traces; see Figure 4 C-D. This result illustrates the incapability of transient absorption in the visible region to detect such a trapping process due to the higher energy carried by the visible probed light, that have the potential to liberate the trapped carriers into higher excited state, producing undistinguishable signal for the trapping process in the visible region.

Conclusion

We show for the first time that transient absorption in the mid-IR region, where charge dynamics of perovskite films can be solely monitored by following the electrons in the conduction band without other contributions of other species. Significantly, the selected region of the mid-IR spectrum can be utilized to follow the actual trapping process of electrons by detecting the negative appearance of the transient signal. We also figure out that similar measurements in the visible region could not be monitored due the energy of the probed light that can liberate the trapped carriers into higher excitation levels, providing additional complexity to distinct between tarped carriers and other species such as excitons and free carriers absorption.

Acknowledgments

The research reported in this publication was supported by funding from King Abdullah University of Science and Technology (KAUST).

References

1 . Alarousu, E.; El-Zohry, A. M.; Yin, J.; Zhumekenov, A. A.; Yang, C.; Alhabshi, E.; Gereige, I.; AlSaggaf, A.; Malko, A. V.; Bakr, O. M.; Mohammed, O. F., Ultralong Radiative States in Hybrid Perovskite Crystals: Compositions for Submillimeter Diffusion Lengths. *JPCL* **2017**, *8*, 4386-4390.

2 . Guo, Z.; Wan, Y.; Yang, M. J.; Snaider, J.; Zhu, K.; Huang, L. B., Long-Range Hot-Carrier Transport in Hybrid Perovskites Visualized by Ultrafast Microscopy. *Science* **2017**, *356*, 59-62.

3 . Zuo, Z. Y.; Ding, J. X.; Zhao, Y.; Du, S. J.; Li, Y. F.; Zhan, X. Y.; Cui, H. Z., Enhanced Optoelectronic Performance on the (110) Lattice Plane of an $Mapbbr_3$ Single Crystal. *J. Phys. Chem. Lett.* **2017**, *8*, 684-689.
4 . Bi, D., et al., Efficient Luminescent Solar Cells Based on Tailored Mixed-Cation Perovskites. *Science Advances* **2016**, *2*.
5 . Kadro, J. M.; Pellet, N.; Giordano, F.; Ulianov, A.; Muntener, O.; Maier, J.; Gratzel, M.; Hagfeldt, A., Proof-of-Concept for Facile Perovskite Solar Cell Recycling. *Energ Environ Sci* **2016**.
6 . Colella, S.; Mazzeo, M.; Rizzo, A.; Gigli, G.; Listorti, A., The Bright Side of Perovskites. *JPCL* **2016**, *7*, 4322-4334.
7 . Zhai, Y. X.; Sheng, C. X.; Zhang, C.; Vardeny, Z. V., Ultrafast Spectroscopy of Photoexcitations in Organometal Trihalide Perovskites. *Adv. Funct. Mater.* **2016**, *26*, 1617-1627.
8 . Shi, D.; Adinolfi, V.; Comin, R.; Yuan, M.; Alarousu, E.; Buin, A.; Chen, Y.; Hoogland, S.; Rothenberger, A.; Katsiev, K., Low Trap-State Density and Long Carrier Diffusion in Organolead Trihalide Perovskite Single Crystals. *Science* **2015**, *347*, 519-522.
9 . Huang, J.; Shao, Y.; Dong, Q., Organometal Trihalide Perovskite Single Crystals: A Next Wave of Materials for 25% Efficiency Photovoltaics and Applications Beyond? *JPCL* **2015**, *6*, 3218-3227.
10 . Fang, H. H.; Raissa, R.; Abdu-Aguye, M.; Adjokatse, S.; Blake, G. R.; Even, J.; Loi, M. A., Photophysics of Organic-Inorganic Hybrid Lead Iodide Perovskite Single Crystals. *Adv. Funct. Mater.* **2015**, *25*, 2378-2385.
11 . Green, M. A.; Bein, T., Photovoltaics Perovskite Cells Charge Forward. *Nature Materials* **2015**, *14*, 559-561.
12 . Gao, P.; Gratzel, M.; Nazeeruddin, M. K., Organohalide Lead Perovskites for Photovoltaic Applications. *Energ Environ Sci* **2014**, *7*, 2448-2463.
13 . Stranks, S. D.; Eperon, G. E.; Grancini, G.; Menelaou, C.; Alcocer, M. J. P.; Leijtens, T.; Herz, L. M.; Petrozza, A.; Snaith, H. J., Electron-Hole Diffusion Lengths Exceeding 1 Micrometer in an Organometal Trihalide Perovskite Absorber. *Science* **2013**, *342*, 341-344.
14 . Meggiolaro, D.; Motti, S. G.; Mosconi, E.; Barker, A. J.; Ball, J.; Perini, C. A. R.; Deschler, F.; Petrozza, A.; De Angelis, F., Iodine Chemistry Determines the Defect Tolerance of Lead-Halide Perovskites. *Energ Environ Sci* **2018**, *11*, 702-713.
15 . Fang, H.-H.; Adjokatse, S.; Wei, H.; Yang, J.; Blake, G. R.; Huang, J.; Even, J.; Loi, M. A., Ultrahigh Sensitivity of Methylammonium Lead Tribromide Perovskite Single Crystals to Environmental Gases. *Science Advances* **2016**, *2*.
16 . Munson, K. T.; Kennehan, E. R.; Doucette, G. S.; Asbury, J. B., Dynamic Disorder Dominates Delocalization, Transport, and Recombination in Halide Perovskites. *Chem* **2018**, *4*, 2826-2843.
17 . Munson, K. T.; Grieco, C.; Kennehan, E. R.; Stewart, R. J.; Asbury, J. B., Time-Resolved Infrared Spectroscopy Directly Probes Free and Trapped Carriers in Organo-Halide Perovskites. *ACS Energy Lett.* **2017**, *2*, 651-658.
18 . Leblebici, S. Y., et al., Facet-Dependent Photovoltaic Efficiency Variations in Single Grains of Hybrid Halide Perovskite. *Nature Energy* **2016**, *1*.
19 . Simpson, M. J.; Doughty, B.; Yang, B.; Xiao, K.; Ma, Y.-Z., Imaging Electronic Trap States in Perovskite Thin Films with Combined Fluorescence and Femtosecond Transient Absorption Microscopy. *JPCL* **2016**, *7*, 1725-1731.

20 . Yamakata, A.; Ishibashi, T.; Onishi, H., Time-Resolved Infrared Absorption Spectroscopy of Photogenerated Electrons in Platinized Tio2 Particles. *Chem. Phys. Lett.* **2001**, *333*, 271-277.
21 . Guo, P. J., et al., Infrared-Pump Electronic-Probe of Methylammonium Lead Iodide Reveals Electronically Decoupled Organic and Inorganic Sublattices. *Nat. Commun.* **2019**, *10*.
22 . Yin, J.; Yang, H.; Song, K.; El-Zohry, A. M.; Han, Y.; Bakr, O. M.; Bredas, J. L.; Mohammed, O. F., Point Defects and Green Emission in Zero-Dimensional Perovskites. *J. Phys. Chem. Lett.* **2018**, *9*, 5490-5495.
23 . Sarmah, S. P., et al., Double Charged Surface Layers in Lead Halide Perovskite Crystals. *Nano Lett* **2017**, *17*, 2021-2027.
24 . Abdellah, M.; El-Zohry, A. M.; Antila, L. J.; Windle, C. D.; Reisner, E.; Hammarström, L., Time-Resolved Ir Spectroscopy Reveals a Mechanism with Tio2 as a Reversible Electron Acceptor in a Tio2–Re Catalyst System for Co2 Photoreduction. *J. Am. Chem. Soc.* **2017**, *139*, 1226-1232.
25 . Asbury, J. B.; Ellingson, R. J.; Ghosh, H. N.; Ferrere, S.; Nozik, A. J.; Lian, T. Q., Femtosecond Ir Study of Excited-State Relaxation and Electron-Injection Dynamics of Ru(Dcbpy)(2)(Ncs)(2) in Solution and on Nanocrystalline Tio2 and Al2o3 Thin Films. *J. Phys. Chem. B* **1999**, *103*, 3110-3119.
26 . Furube, A.; Murai, M.; Watanabe, S.; Hara, K.; Katoh, R.; Tachiya, M., Near-Ir Transient Absorption Study on Ultrafast Electron-Injection Dynamics from a Ru-Complex Dye into Nanocrystalline In2o3 Thin Films: Comparison with Sno2, Zno, and Tio2 Films. *J Photoch Photobio A* **2006**, *182*, 273-279.
27 . Ellingson, R. J.; Asbury, J. B.; Ferrere, S.; Ghosh, H. N.; Sprague, J. R.; Lian, T. Q.; Nozik, A. J., Dynamics of Electron Injection in Nanocrystalline Titanium Dioxide Films Sensitized with [Ru(4,4 '-Dicarboxy-2,2 '-Bipyridine)(2)(Ncs)(2)] by Infrared Transient Absorption. *J. Phys. Chem. B* **1998**, *102*, 6455-6458.
28 . El-Zohry, A. M., The Origin of Slow Electron Injection Rates for Indoline Dyes Used in Dye-Sensitized Solar Cells. *Dyes Pigm.* **2019**, *160*, 671-674.
29 . El-Zohry, A. M.; Karlsson, M., Gigantic Relevance of Twisted Intramolecular Charge Transfer for Organic Dyes Used in Solar Cells. *J. Phys. Chem. C* **2018**, *122*, 23998-24003.
30 . Juozapavicius, M.; Kaucikas, M.; Dimitrov, S. D.; Barnes, P. R. F.; van Thor, J. J.; O'Regan, B. C., Evidence for "Slow" Electron Injection in Commercially Relevant Dye-Sensitized Solar Cells by Vis-Nir and Ir Pump-Probe Spectroscopy. *J. Phys. Chem. C* **2013**, *117*, 25317-25324.
31 . Juozapavicius, M.; Kaucikas, M.; van Thor, J. J.; O'Regan, B. C., Observation of Multiexponential Pico- to Subnanosecond Electron Injection in Optimized Dye-Sensitized Solar Cells with Visible-Pump Mid-Infrared-Probe Transient Absorption Spectroscopy. *J. Phys. Chem. C* **2012**, *117*, 116-123.
32 . Ghosh, H. N.; Asbury, J. B.; Lian, T. Q., Direct Observation of Ultrafast Electron Injection from Coumarin 343 to Tio2 Nanoparticles by Femtosecond Infrared Spectroscopy. *J. Phys. Chem. B* **1998**, *102*, 6482-6486.
33 . El-Zohry, A. M.; Zietz, B., Electron Dynamics in Dye-Sensitized Solar Cells Influenced by Dye-Electrolyte Complexation. *J. Phys. Chem. C* **2020**, *124*, 16300-16307.
34 . Furube, A.; Du, L.; Hara, K.; Katoh, R.; Tachiya, M., Ultrafast Plasmon-Induced Electron Transfer from Gold Nanodots into Tio2 Nanoparticles. *J. Am. Chem. Soc.* **2007**, *129*, 14852-14855.

35 . Pavliuk, M. V.; Fernandes, D. L. A.; El-Zohry, A. M.; Abdellah, M.; Nedelcu, G.; Kovalenko, M. V.; Sa, J., Magnetic Manipulation of Spontaneous Emission from Inorganic Cspbbr3 Perovskites Nanocrystals. *Advanced Optical Materials* **2016**, *4*, 2004-2008.
36 . Cieslak, A. M., et al., Ultra Long-Lived Electron-Hole Separation within Water-Soluble Colloidal Zno Nanocrystals: Prospective Applications for Solar Energy Production. *Nano Energy* **2016**, *30*, 187-192.
37 . Harrick, N. J., Lifetime Measurements of Excess Carriers in Semiconductors. *J. Appl. Phys.* **1956**, *27*, 1439-1442.
38 . Tang, J., et al., Colloidal-Quantum-Dot Photovoltaics Using Atomic-Ligand Passivation. *Nature Materials* **2011**, *10*, 765-771.
39 . Heimer, T. A.; Heilweil, E. J., Direct Time-Resolved Infrared Measurement of Electron Injection in Dye-Sensitized Titanium Dioxide Films. *J. Phys. Chem. B* **1997**, *101*, 10990-10993.
40 . Guo, P. J., et al., Slow Thermal Equilibration in Methylammonium Lead Iodide Revealed by Transient Mid-Infrared Spectroscopy. *Nat. Commun.* **2018**, *9*.
41 . El-Zohry, A. M.; Cong, J.; Karlsson, M.; Kloo, L.; Zietz, B., Ferrocene as a Rapid Charge Regenerator in Dye-Sensitized Solar Cells. *Dyes Pigm.* **2016**, *132*, 360-368.
42 . Barker, A. J., et al., Defect-Assisted Photoinduced Halide Segregation in Mixed-Halide Perovskite Thin Films. *ACS Energy Lett.* **2017**, *2*, 1416-1424.
43 . Samu, G. F.; Janáky, C.; Kamat, P. V., A Victim of Halide Ion Segregation. How Light Soaking Affects Solar Cell Performance of Mixed Halide Lead Perovskites. *ACS Energy Lett.* **2017**, *2*, 1860-1861.